Catching the Sounds of Stars

ASTEROSEISMOLOGY, THE RIGHT TOOL TO UNDERSTAND STELLAR INTERIORS

F. BOUCHY, F. CARRIER

Contact e-mail: francois.bouchy@obs.unige.ch
Observatoire de Genève, Switzerland

1. Why Measure Stellar Acoustic Oscillations?

The physics of stellar interiors is poorly known. There are serious uncertainties about the modelling of the inner structure and about the stellar evolution. The main problem is the lack of observational constraints. We have usually only two observables: the effective temperature and the luminosity. In some cases, the detailed analysis of the spectrum allows us to determine surface abundances and to estimate surface gravity. However, all these observables trace only the physical conditions prevailing in a thin layer of the stellar internal structure, the photosphere. Masses and radius are known for a limited number of double systems. As a consequence, the stellar internal structure and the evolution theory is not well tested.

Geologists learn about the inner structure of our planet by monitoring how seismic waves generated by earthquakes propagate through the Earth. In a way, they show us the method needed to study the inside of a star. By chance almost every star undergoes perturbations that generate seismic waves (see Fig. 1). The principle is to detect and measure seismic oscillation modes of a star in order to understand its inner structure.

2. Acoustic Spectrum of Solar-like Stars

The discovery of the propagating sound waves in the Sun by Leighton et al. (1962) and their interpretation by Ulrich (1970) has opened a new area in stellar physics. Since the Sun is a sphere of hot gas, its interior transmits acoustic waves very well. Convection near the stellar surface produces vigorous turbulent flows that generate a broad spectrum of random acoustical waves. The process of destructive and constructive interferences transforms this random convective noise into a very rich acoustic spectrum in the subaudible domain with periods of few minutes (see Fig. 2). The resulting oscillations are pressure waves, also called p-modes. Each acoustic eigenmode is trapped in a spherical-shell cavity between the stellar surface and a specific inner layer. Frequencies and amplitudes of these oscillation modes depend on the physical conditions prevailing in the layers crossed by the waves and provide a powerful seismological tool. Helioseismology led to major revisions in the "standard model" of the Sun and provided for instance measures of the sun's inner rotation, the size of the convective zone and the structure of the external layers.

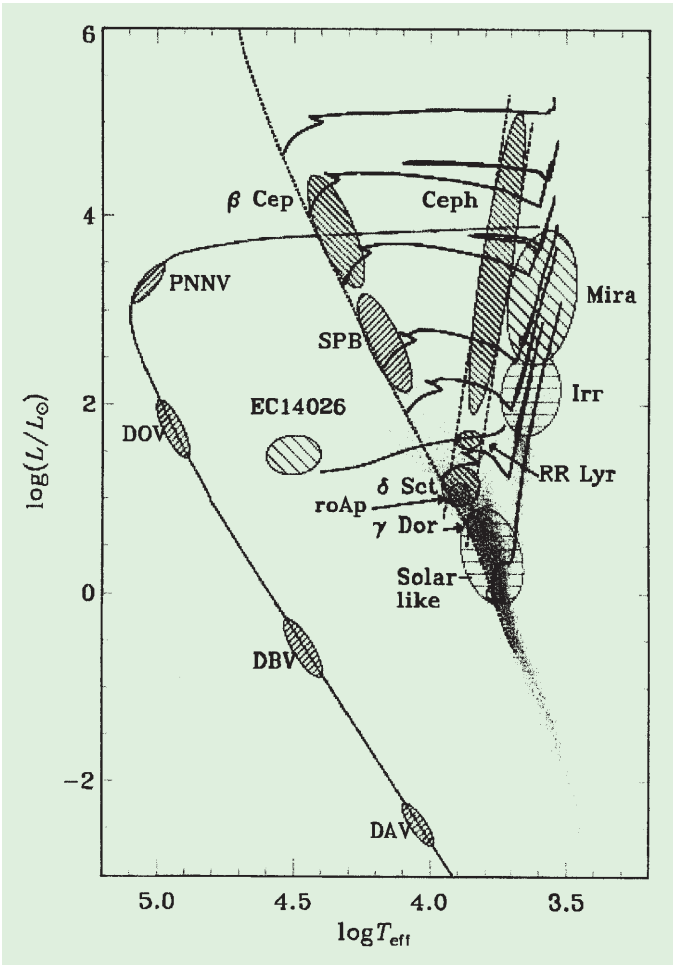

Figure 1: Schematic location of classes of pulsating stars in the HR diagram. Solar-like stars correspond to stars with intermediate masses near the main sequence. This class undergoes nonradial oscillations generated by the stochastic excitation of their outer convective zone.

Each oscillation mode can be characterised by the two quantum numbers *n* and *l* which are respectively the radial order (see footnote number 1) and the angular degree (see footnote number 2) of modes. In stars where the disk is not resolved, it is only possible to measure the lowest-degree modes ($l \leq 3$). Fortunately, these modes are especially interesting because they penetrate more deeply into the stellar interior and probe the physical conditions near the stellar core. The p-mode oscillations produce a characteristic comb-like structure in the power spectrum with mode frequencies $\nu_{n,l}$ well approximated by the asymptotic relation:

$$\nu_{n,l} = \Delta\nu_0(n + l/2 + \epsilon) - l(l+1)\delta\nu_0/6$$

The parameters $\Delta\nu_0$, ε and $\delta\nu_0$ are related to the stellar structure. The large separation $\Delta\nu_0$ reflects the average stellar density while ε is related to the physical conditions at the boundaries of the acoustic cavity and therefore it is sensitive to physical conditions in the surface layers. The small separation $\delta\nu_0$ depends on the mean molecular weight down to the central regions of the star and it is thus an indicator of the stellar age. A considerable advantage of the asteroseismology comes from the fact that the measurement of the frequencies $\nu_{n,l}$ and their amplitudes A_{osc} allows to constrain directly the internal structure of models independently of any intermediate steps like radiation transfer in the atmosphere or photometric calibrations.

The oscillation characteristics of solar-like stars are expected in first approximation to scale from solar values (Kjeldsen & Bedding 1995) as a func-

[1]Number of nodes in the radial direction.
[2]Number of nodes around a circumference.

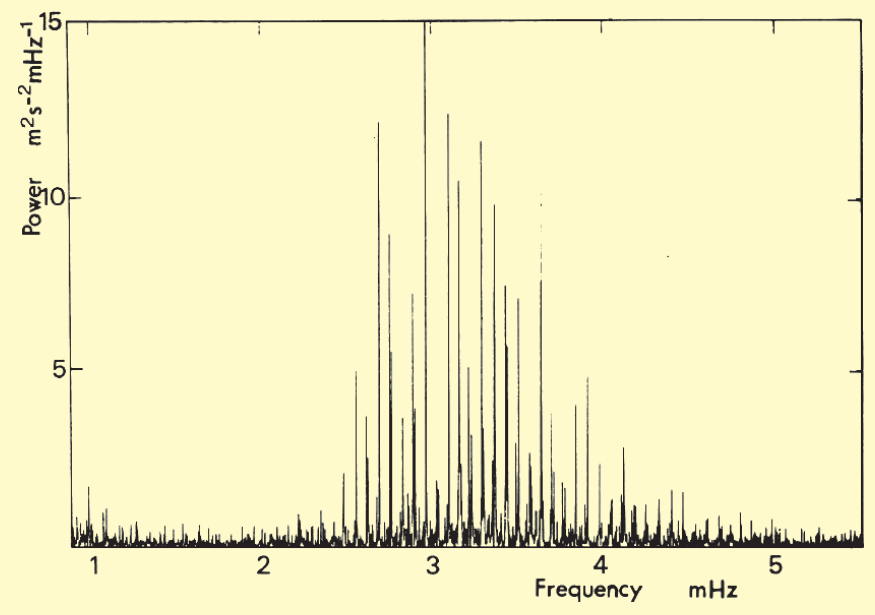

Figure 2: Acoustic spectrum of the full solar disk (Grec et al. 1983) showing the presence of several tens of eigen frequencies with periods in the range 3 to 8 minutes. The individual Doppler amplitudes of these acoustic modes are lower than 25 cm s^{-1}.

tion of the stellar luminosity (or radius), mass and temperature according to:

$$A_{osc} = \frac{L/L_\odot}{M/M_\odot} 23.4\ cm\ s^{-1},$$

$$\nu_{max} = \frac{M/M_\odot}{(R/R_\odot)^2 \sqrt{Teff/5777K}} 3.05\ mHz,$$

$$\Delta\nu_0 = \frac{(M/M_\odot)^{1/2}}{(R/R_\odot)^{3/2}} 134.9\ \mu Hz.$$

Solar-like oscillation modes generate periodic motions of the stellar surface (see Fig. 3) with periods in the range 3–30 mn but with extremely small amplitudes. Essentially two methods exist to detect such a motion: photometry and Doppler spectroscopy. In photometry, the amplitudes of the oscillation of solar-like stars are in the range 2–20 ppm (see footnote number 3) while they are in the range 10–100 cm s^{-1} in radial velocity measurements. Photometric measurements made from ground are strongly limited by scintillation noise. To reach the needed accuracy it actually requires measurements made from space. The accuracy of Doppler spectroscopy has recently been improved, mostly driven by intensive search for extra-solar planet programmes. Actually they have reached the accuracy needed to detect p-mode oscillations from the ground on bright solar-like stars.

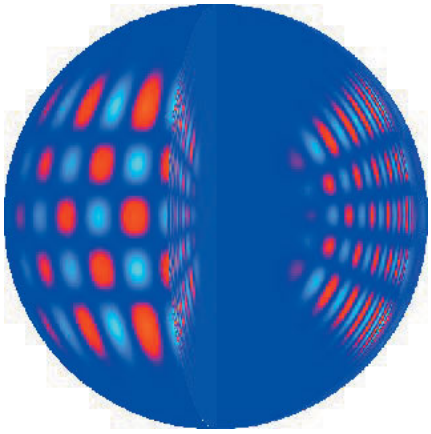

Figure 3: Representation of resonating acoustic waves in the interior of a solar-like star. Red and blue colours show the displacement of elements in opposite directions.

[3]Part per million or 10^{-6} L where L is the stellar luminosity.

3. Listen to Solar-like Stars by Precise Doppler Measurements

The detection of acoustic oscillations of stars needs long and intensive sequences of high-precision radial velocity measurements. In order to reach a precision of few m s^{-1} one needs first high flux and enough spectral information to compute the radial velocity without being limited by photon noise. Second, a stable wavelength reference is necessary to measure and to correct systematic errors of the spectrograph. The photon noise limit depends on the wavelength spectral range and on the spectral resolution of the spectrograph. It depends as well on the spectral type and the rotational broadening *v* sin *i* (see footnote number 4) of the star. A detailed analysis of the fundamental photon noise limit on radial velocity measurements can be found in Bouchy et al. (2001). For illustration, Figure 4 shows the expected radial velocity errors with the high-resolution echelle spectrograph CORALIE (Queloz et al. 2001) for a 100 s exposure time on a 5th-magnitude star versus effective temperature and rotational broadening.

Essentially two different methods can be used to gather precise Doppler measurements (see Fig. 5). Both mon-

[4]Equatorial stellar velocity projected on the line of sight causing Doppler broadening of the stellar lines.

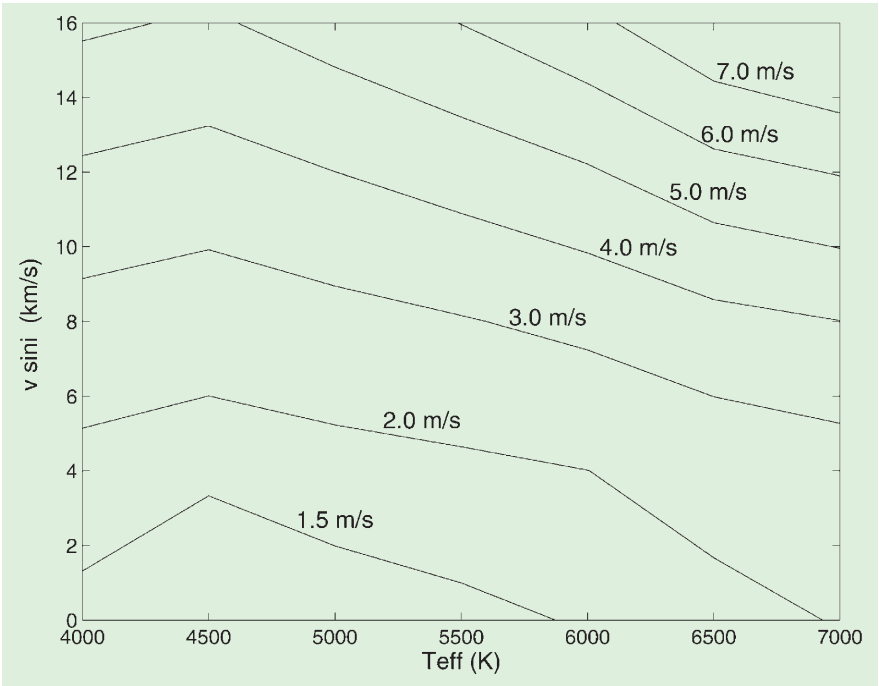

Figure 4: Radial velocity uncertainty predictions for the spectrograph CORALIE for a flux given by t_{exp} (s) = 2.512^{mv}. This spectrograph, installed on the Euler 1.2-m telescope, covers a spectral range of 3000 Å with a resolution of 50,000 and a total efficiency peak of 1.5%.

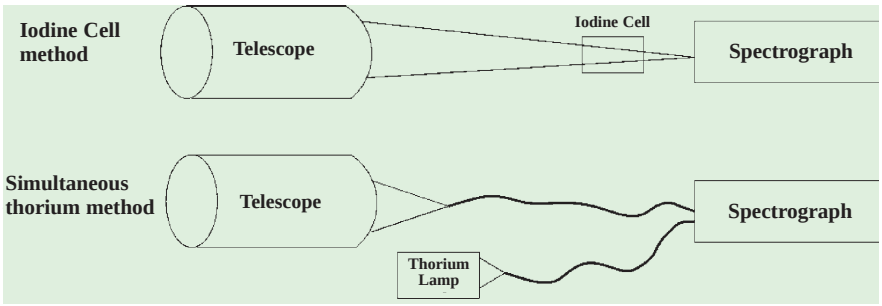

Figure 5: The different methods of radial velocity measurements.

itor instrumental changes by comparison with a set of stable reference lines. One method, called the Iodine cell method, inserts in the input stellar beam an iodine cell to impress stable absorption lines on the incoming starlight. Another method, called the simultaneous thorium method, uses an optical fibre for the star light, in conjunction with a second fibre carrying light from a thorium lamp. A variant consists in replacing the thorium lamp by a fixed Fabry-Perot interferometer illuminated by a white lamp. Both methods have recently shown precision of only few m s^{-1}. However, although very reliable, the iodine cell approach increases the photon noise errors by limiting the spectral range to about 1000 Å and reducing the total efficiency by a factor of ~ 2. Hence, for a given photon noise limit, this technique requires telescopes at least 2 times larger than for an instrument using the simultaneous thorium method.

Even if the precision of individual measurements of the radial velocity is greater than 1 m s^{-1}, periodic Doppler variations as small as 10 cm s^{-1} can be detected if a large amount of measurements is made. The relation between mean noise level in the power spectrum σ_{PS} and the dispersion of the time series Doppler measurements σ_{obs} is given by:

$$\sigma_{PS} = \frac{4\,\sigma_{obs}^2}{N},$$

where *N* is the number of measurements. If the noise is Gaussian then the mean noise level in the amplitude spectrum σ_{amp} *is* given by:

$$\sigma_{amp} = \sqrt{\frac{\pi\,\sigma_{PS}}{4}}.$$

For example, 400 measurements with 2 m s^{-1} precision allow us to reach a noise level in the amplitude spectrum of 18 cm s^{-1}.

The difficulty is not only to reach a high signal-to-noise level but to have a sufficiently long duration of observation to resolve and to characterise the eigen frequencies with sufficient accuracy. For example, in the Sun, the small separation $\delta\nu_0$ is equal to about 9 μHz. The solar oscillation modes are broadened by their limited lifetime (few days) and have a typical mean width of about 2 μHz. For these reasons, one needs frequency resolution at least equal to 2 μHz to characterise the acoustic modes with accuracy. This implies a duration of observation at least equal to 6 nights.

Figure 6: α Cen A is the brightest star of the picture. One can see the Southern Cross on the left.

With single-site observations, the identification of oscillation modes can be complicated by the observation window limited by the diurnal cycle. Each mode in the power spectrum presents the day aliasings at 11.57 μHz. In order to improve the spectral window and reduce these aliases, it is useful to realise multi-longitude observations as they already exist for helioseismology (IRIS, BiSON, GONG, see Pallé 1997).

4. Recent Progress in Solar-like Seismology

Many attempts to detect signature of p-mode oscillations on solar-like stars have been made since the 1980's. Until 1999, they reached only upper limits or the detections were not very reliable.

The first good evidence of excess power due to mode oscillations was obtained by Martic et al. (1999) on the F5 subgiant Procyon. Bedding et al. (2001) obtained a quite similar excess power on the G2 subgiant β Hyi, an evolved solar-mass star that corresponds to the future evolution of the Sun. These two results have been confirmed independently by our group based on observations made with the CORALIE spectrograph (Carrier et al. 2001a, 2001b).

A primary and challenging target for the search for p-mode oscillations was the nearby solar twin Rigil Centaurus (α Cen A). In May 2001, we made for the first time on this star an unambiguous detection of solar-like acoustic modes (Bouchy & Carrier 2001; Carrier et al. 2001c). The observations and analysis are presented in the next section.

The main parameters of these three stars, Procyon, β Hyi and α Cen *A,* and the characteristic of their observed seismic signal are reported in Table 1 and are compared with the Sun.

The seismic parameters of these three stars are in agreement with the expected values scaled from the Sun. So far the low signal to noise obtained and the day aliasings coming from the single-site window function have not allowed to identify modes on Procyon and β Hyi. On α Cen A, the high signal to noise obtained and the fact that modes are more separated in frequency and less sensible to the day aliasings, allow to identify them.

Table 1: Main parameters of the solar-like stars where seismological signal was obtained.

	Sun	α CMi HR2943	β Hyi HR98	α Cen A HR5459
Spectral type	G2V	F5IV-V	G2IV	G2V
mv	–27	0.34	2.80	0.0
T_{eff} (K)	5777	6530	5800	5780
$L/L_\odot$	1	7.1	3.5	1.5
$M/M_\odot$	1	1.5	1.1	1.12
A_{osc} (cm s^{-1})	23.4	50	50	31
ν_{max} (mHz)	3.05	1	1.1	2.3
$\Delta\nu_0$ (μHz)	134.9	55	58	105.5
$\delta\nu_0$ (μHz)	9	–	–	6.6

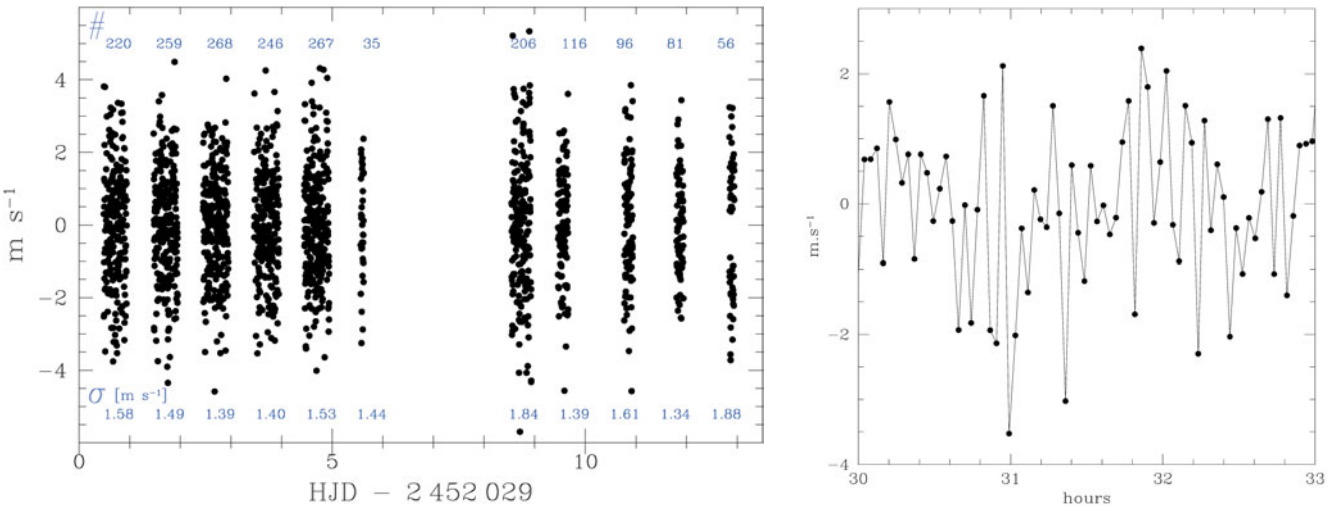

Figure 7: Left: Radial velocity measurements of the star α Cen A. A 3-order polynomial fit subtraction was applied on each night. The number of Doppler measurements and their dispersion are indicated for each night. Right: Portion of 3 hours of the radial velocity measurements obtained during the third night. On this part the dispersion reaches 1.25 m s^{-1}.

5. Acoustic Waves in Solar-twin α Cen A

5.1 Observations

The star α Cen A (see Fig. 6) was observed with the CORALIE fibre-fed echelle spectrograph (Queloz et al. 2000) mounted on the 1.2-m Swiss telescope at the ESO La Silla Observatory. CORALIE is the southern hemisphere twin of the ELODIE spectrograph (Baranne et al. 1996), both of them well known for their discoveries of extra-solar planets. The wavelength domain ranges from 3875 to 6820 Å recorded on 68 orders. Using a 2k by 2k CCD with 15-μm pixels, CORALIE reaches a spectral resolution of 50,000 with 3-pixel sampling. The total efficiency including atmosphere, telescope, spectrograph and detector reaches about 1.5% at 5500 Å in the best seeing case. During stellar exposures, the spectrum of a thorium lamp carried by a second fibre is simultaneously recorded in order to monitor the spectrograph instability and thus to obtain high-precision velocity measurements.

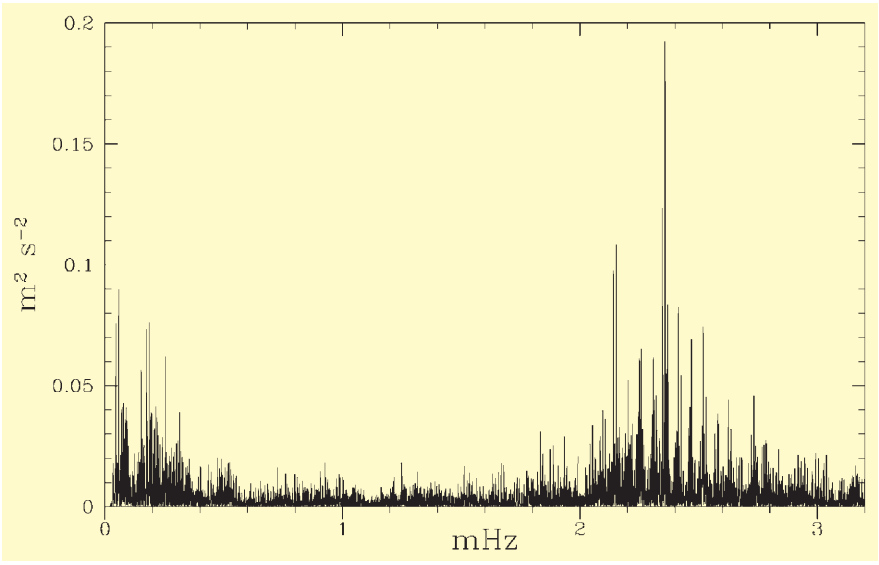

Figure 8: Power spectrum of 13 nights of radial velocity measurements of the star α Cen A. The series of peaks between 1.8 and 2.9 mHz is the unambiguous signature of solar-like oscillations.

α Cen A was observed over 13 nights in May 2001. Exposure time was 40 s, with a dead time of 110 s between exposure. In total, 1850 spectra were collected with typical signal-to-noise ratio

Table 2: Mode frequencies (in μHz). The frequency resolution of the time series is 0.9 μHz. The last row shows the average large spacing $\Delta\nu_{n,l} = \nu_{n,l} - \nu_{n-1,l}$ computed for l = 0, 1 and 2.

	l = 0	l = 1	l = 2
n = 15			1833.0
n = 16	1841.2	1887.2	1935.0
n = 17		1991.9	2041.5
n = 18		2095.6	2145.9
n = 19	2152.8	2202.8	2251.3
n = 20	2258.3	2308.9	2358.3
n = 21	2364.2	2414.2	2464.1
n = 22	2470.0	2519.3	2568.5
n = 23	2573.2	2625.5	2672.2
n = 24	2679.7	2733.0	2782.9
n = 25		2837.4	
$\Delta\nu_0$	105.4 ± 0.5	105.6 ± 0.4	105.5 ± 0.8

Table 3: Upper panel: Observational constraints adopted for the calibration of models. Lower Panel: Global characteristics derived from the calibrated models.

Models	A_{BV}, A_{ov} & A_{CM}	A_{GD}
$M/M_\odot$	1.16 ± 0.031	1.1015 ± 0.008
T_{eff} [K]	5790 ± 30	5770 ± 50
log *g*	4.32 ± 0.05	4.28 ± 0.02
$[\frac{Fe}{H}]_i$	0.20 ± 0.02	0.22 ± 0.02
$L/L_\odot$	1.534 ± 0.103	1.572 ± 0.135

Models	A_{BV}	A_{ov}	A_{CM}	A_{GD}
t [*Myr*]	2710	3530	4086	5640
Y_i	0.284	0.279	0.271	0.300
$(\frac{Z}{X})_i$	0.0443	0.0450	0.0450	0.0480
α	1.53	1.64	0.96	1.86

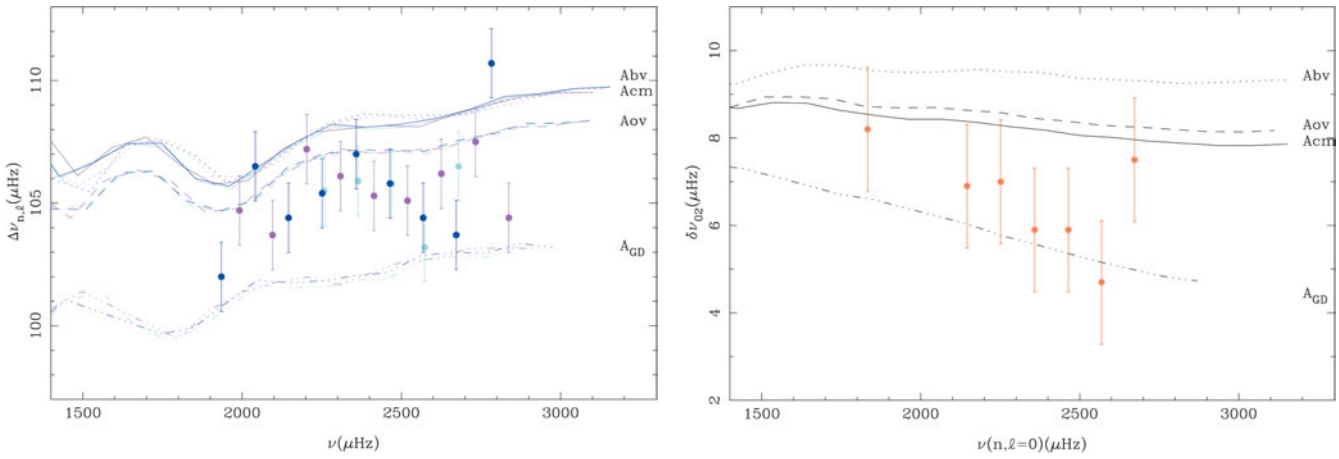

Figure 9: Left: Variations of the large spacing between modes of consecutive radial order $\Delta\nu_{n,l} = n_{n,l} - \nu_{n-1,l}$ for p-modes of degree l = 0 (light blue line), l = 1 (purple line) and l = 2 (dark blue line) versus frequency. Right: Variations of the small frequency spacing $\delta\nu_{02} = \nu_{n,0} - \nu_{n-1,2}$ versus frequency.

in the range 300–420 at 550 nm. The data reduction, based on the optimum-weight procedure, is described in Bouchy et al. (2001). The resulting velocities are presented in Figure 7. The dispersion of these measurements reaches 1.53 m s^{-1}. The photon noise uncertainties coming from the stellar spectrum and from the simultaneous thorium spectrum used in the instrumental tracking are typically the same and equal to 0.50 m s^{-1}. The quadratic sum of these two photon noise contributions is 0.70 m s^{-1}.

5.2 Acoustic spectrum analysis

The power spectrum shown in Figure 8 exhibits a series of peaks between 1.8 and 2.9 mHz modulated by a broad envelope. This is the typical signature of solar-like oscillations and can be compared with the acoustic spectrum of the Sun in Figure 2.

Toward the lowest frequencies (ν < 0.6 mHz), the power rises and scales inversely with frequency squared as expected for instrumental instabilities. The mean white noise level σ_{PS}, computed in the range 0.6–1.5 mHz reaches 2.39 × 10^{-3} m^2 s^{-2}, namely 4.3 cm s^{-1} in amplitude. This noise level corresponds to a velocity accuracy of 1.05 m s^{-1} which is to be compared with the estimated photon noise uncertainty of about 0.70 m s^{-1}. The average amplitude of the highest modes is estimated in the range 29–33 cm s^{-1}.

The strongest identified modes are listed in Table 2. The values of *n* and *l* are deduced from the asymptotic relation with parameter ε estimated to 1.41.

The average large and small spacing are deduced from this table:

$$< \Delta\nu_0 > = < \nu_{n,l} - \nu_{n-1,l} > = 105.5 \pm 0.3\ \mu Hz,$$

$$< \delta\nu_0 > = < \nu_{n,0} - \nu_{n-1,2} > = 6.6 \pm 0.4\ \mu Hz.$$

The modes corresponding to *l* = 3 are expected to be separated by about 11 μHz to the modes *l* = 1. This expected separation is near the day aliasing at 11.57 μHz and explains why they cannot be identified.

5.3 Astrophysical interpretation

The variation with the frequency of the large and small spacings obtained from our observations are compared in Figure 9 with the values deduced from three models developed by Morel et al. (2000) (A_{BV}, A_{ov} and A_{CM}) and one model developed by Guenther & Demarque (2000) (A_{GD}) The observational constraints for the model calibrations and the properties of the calibrated models are given in Table 3. The two sets of models differ essentially by the estimated mass and the age of the star.

For α Cen A, our observations clearly suggest a model with properties intermediate between the two sets of models, i.e. a mass near 1.13 $M_\odot$. The age of αCen A seems to be close to 5 Gyr. New models of α Cen A are presently developped by the OCA team (Provost, Berthomieu, Morel and Thevenin) with different properties in order to better interpret the observed oscillations.

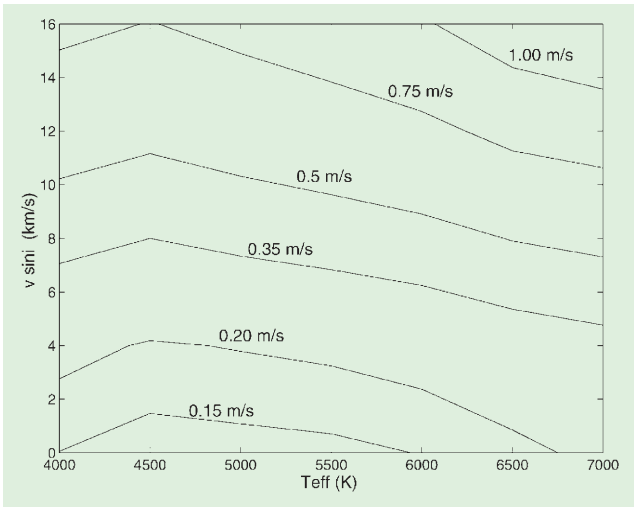

Figure 10: Radial velocity uncertainty predictions for the spectrograph HARPS for a flux given by t_{exp} (s) = 2.512^{mv}. This spectrograph, installed at the ESO 3.6-m telescope, covers a spectral range of 3000 Å with a resolution of 90,000 and a total efficiency peak of 4.5%.

6. Future Prospects with ESO Instruments

This result on a Cen A demonstrates the power of the simultaneous thorium radial velocity method and shows that Doppler asteroseismology can be further developed from the ground. With the CORALIE spectrograph installed on a small 1.2-m telescope, we are limited to observe targets brighter than 3rd or 4th magnitude. But ESO has developed and develops spectrographs fully adapted for Doppler asteroseismology.

The FEROS spectrograph based on the 1.52-m telescope at La Silla observatory has recently shown its capability to obtain high-precision radial velocity measurements (Setiawan et al. 2000) with the simultaneous thorium method. Considering its very high efficiency, the estimated gain is 2 magnitude compared to CORALIE.

The state of the art will be the future spectrograph HARPS (High Accuracy Radial velocity Planetary Searcher) which will be installed on the 3.6-m ESO telescope at La Silla observatory (Queloz et al. 2001). This instrument is optimised and dedicated to high-precision radial velocity measurements and it is designed to reach 1 m s^{-1} precision. A detailed photon noise study for HARPS can be found in Bouchy et al. (2001). The expected radial velocity errors due to the photon noise for a 100 s exposure time on a 5th-magnitude star

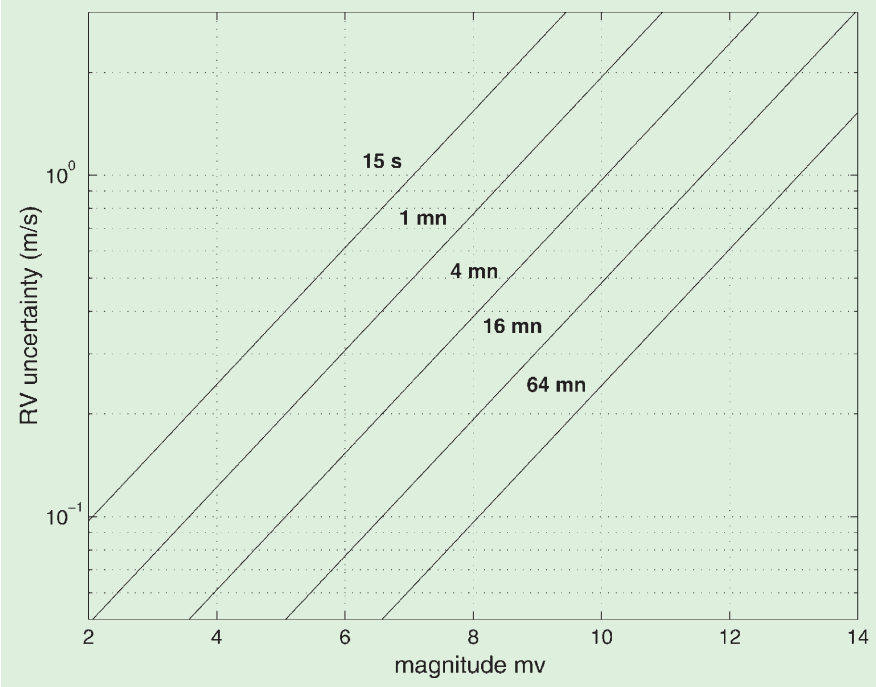

Figure 11: Radial velocity uncertainty predictions for HARPS versus magnitude for a star spectrum with T_{eff} = 4500 K and v sin i = 0 km s^{-1}.

is presented in Figure 10 versus effective temperature and rotational broadening. Figure 11 shows the photon noise uncertainty versus stellar magnitude for the best stellar case (T_{eff} = 4500 K, *v* sin *i* = 0 km s^{-1}) for various exposure times. This quantity is less than 1 m s^{-1} for exposure time of 1 mn on stars with magnitude lower than 8. Typically, a gain of 5 magnitudes is expected compared to CORALIE.

UVES (Ultraviolet and Visual Echelle Spectrograph) is a cross-dispersed echelle spectrograph located at the second Unit Telescope of the 8.2-m ESO VLT. FLAMES (Fibre Large Array Multi Element Spectrograph) is a VLT large-field fibre facility that consists of several components, including a fibre link to the UVES spectrograph. The light is collected at the Nasmyth focus through 8 fibres in a usable field of up to 25 arcmin in diameter. Considering that one fibre is used for the simultaneous Thorium spectrum, 7 objects can be simultaneously measured with UVES. The photon-noise study for HARPS has been extrapolated to UVES and shows a gain between 1 and 2 magnitudes.

All these prospects show that Doppler ground-based asteroseismology will undergo intensive developments these next years and will be able to enlarge our understanding on stellar physics.

Acknowledgements

We would like to thank M. Mayor who encourages our programme and gives us time allocation at the Euler Swiss telescope. D. Queloz and all people associated with the CORALIE and HARPS projects are acknowledged for their help and for ongoing discussions and helpful comments.

References

Baranne, A., Queloz, D., Mayor, M., et al., 1996, *A&ASS*, **119**, 373.

Bouchy, F., & Carrier, F., 2001, *A&A*, **374**, L5.

Bouchy, F., Pepe, F., Queloz, D., 2001, *A&A*, **374**, 733.

Bedding, T.R., Butler, R.P., Kjeldsen, H., et al., 2001, *ApJ*, **549**, L105.

Carrier, F., Bouchy, F., Kienzle, F., & Blecha, A., 2001a, IAU 185, ASP Conf. Ser., in press.

Carrier, F., Bouchy, F., Kieuzle, F., et al., 2001b, *A&A*, **378**, 142.

Carrier, F., Bouchy, F., Provost, J., et al., 2001c, IAU 185, ASP Conf. Ser., in press.

Grec, G., Fossat, E., Pomerantz, M.A., 1983, *Solar Physics*, **82**, 55.

Guenther, D.B., & Demarque, P., 2000, *ApJ*, **531**, 503.

Kjeldsen, H., & Bedding, T., 1995, *A&A*, **293**, 87.

Leighton, R.B., Noyes, R.W., & Simon, G.W., 1962, *ApJ*, **135**, 474.

Martic, M., Schmitt, J., Lebrun, J.-C., et al., 1999, *A&A*, **351**, 993.

Morel, P., Provost, J., Lebreton, Y., et al., 2000, *A&A*, **363**, 675.

Pallé, P., 1997, Proc. IAU Symp. 181, Provost & Schmider (eds), 15.

Queloz, D., Mayor, M., Weber, L., et al., 2000, *A&A*, **354**, 99.

Queloz, D., Mayor, M., et al., 2001, *The Messenger*, **105**, 1.

Setiawan, J., Pasquini, L., da Silva, L., et al., 2000, *The Messenger*, **102**, 13.

Ulrich, R.K., 1970, *ApJ*, **162**, 993.

Discovery of Lead Stars with the ESO 3.6-m Telescope and CES

S. VAN ECK (Institut d'Astronomie et d'Astrophysique, Université Libre de Bruxelles), svaneck@astro.ulb.ac.be

S. GORIELY and A. JORISSEN (Institut d'Astronomie, Bruxelles), and B. PLEZ (GRAAL, Montpellier)

1. The Synthesis of Elements Heavier than Iron in Stars

In a seminal paper, Burbidge et al. (1957) lay the foundations of our understanding of the origin of the elements heavier than iron: these elements cannot be formed by the mainstream nucleosynthesis processes feeding the stellar energy. They require instead that pre-existing seed nuclei, like the abundant iron-group elements, form heavier and heavier nuclei by successive captures of neutrons. In this neutron-capture chain, unstable nuclei are formed. Depending on the respective time scales for β-decay and neutron-capture (respectively τ_β and τ_n), the neutron-capture process will either be dubbed slow (s-process: $\tau_\beta < \tau_n$) or rapid (r-process: $\tau_\beta > \tau_n$). The r-process occurs during the supernova event, and is able to produce heavy elements up to the actinides (Th, U). These actinides are injected into the interstellar medium by the supernova remnant, and are subsequently incorporated into the next